

# An Assessment of Structural Optimization Methods for Device-Level Heat Sink Design

Danny J Lohan<sup>1\*</sup>, James T. Allison<sup>1</sup>

<sup>1</sup>Dept. of Industrial and Enterprise Systems Engineering, University of Illinois at Urbana-Champaign, Urbana, USA

\* Corresponding author: dlohan2@illinois.edu

## Abstract

In this research, we investigate the design of heat spreading structures at a power electronic device level using several structural design optimization methods, reduced-order analysis models, boundary conditions, and objective functions. These methods include the Solid Isotropic Microstructure with Penalization (SIMP) method, the differentiable geometric projection method, and a generative method based on the use of the Space Colonization Algorithm. The most promising optimized structures are fabricated using a lost-wax casting approach and their performance is experimentally verified on an electronics test-circuit. It was observed that solutions with simple, straight fin, geometric features outperformed solutions with complex, or dendritic features.

**Keywords:** Heat Transfer, Topology Optimization, Heat Sink Design

## 1. Introduction

Advances in high-band gap devices have enabled the design of high temperature power electronic systems. These systems present new challenges for thermal engineers where devices with both low- and high-temperature sensitivity are placed within a common package. This heterogeneous mix of electronic devices motivates heat removal at a device level to prevent the unintentional failure of nearby devices. Researchers have developed several methods to address the challenge of heat removal using a heat spreading structure for convective cooling. These vary from free-form design driven by a gradient based algorithm [1] to constrained fin design driven by a genetic algorithm [2] using multi-physics simulations. Reduced-order analysis methods have also been developed to decrease the computational expense associated with multi-physics simulation in the context of heat spreader design [3,4]. A general review of topology optimization methods for heat transfer systems is presented in [5].

In this research, we explore several aspects of design problem formulation for reduced-order heat spreading structure design. The target application and associated physics consideration are discussed in the following section. This is followed by short descriptions of the design representations, including topology optimization [6], geometric projection methods [7], and generative design methods [8]. A selection of optimized topologies is presented to show variations in design due to problem formulation considerations. Several of the heat sink designs are then manufactured and their performance is experimentally quantified. A discussion of findings is presented and topics for future work are identified.

## 2. Device-level heat sink design formulation

In this research we are investigating the individualized design of heat spreading structures at an electronic component level. Consider the cross-section of the following electronic board, illustrated in Fig. 1.

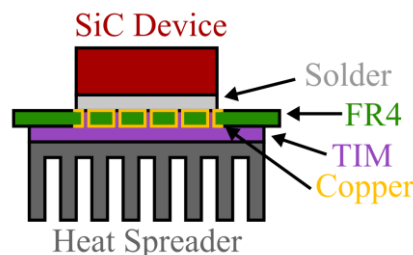


Figure 1. Cross-section of a bottom-cooled SiC MOSFET.

A power electronic device, such as Silicon-Carbide (SiC) MOSFET, is soldered onto copper pads on a printed circuit board (PCB). Typically, heat spreading structures are attached to the top of the device separated by a thermal interface material (TIM). Here we use a specialized device where heat is extracted through the bottom surface of the device. The

heat is transferred through the PCB using copper coated through-silicon-vias to the heat spreading structure mounted on the reverse side of the PCB. A fan will be used to blow air onto the heat spreading structure to remove the heat. This cooling topology presents several advantages, such as alleviating electrical isolation and mechanical stress risks associated with mounting large heat sinks across the top of electronic devices.

The heat spreading mechanism is a function of both conductive and convective heat transfer through the electronic system. Consider the, 20x20x10mm, air volume where the heat spreading structure resides, depicted in Fig. 2. This corresponds to the volume under the PCB shown in Fig. 1. A majority of heat flux will be extracted through the bottom surface of the device (shown in red), and airflow will enter through the right surface of the design volume and exit through the other surfaces as physics dictate. This problem type has been solved for several applications in the literature while accounting for conduction and/or thermo-fluid interactions [5]. The optimization of these systems presents a large computational burden, and there have been several investigations using reduced order models [3, 4]. In this research, we directly compare the effect of using various reduced-order models for the heat sink design task.

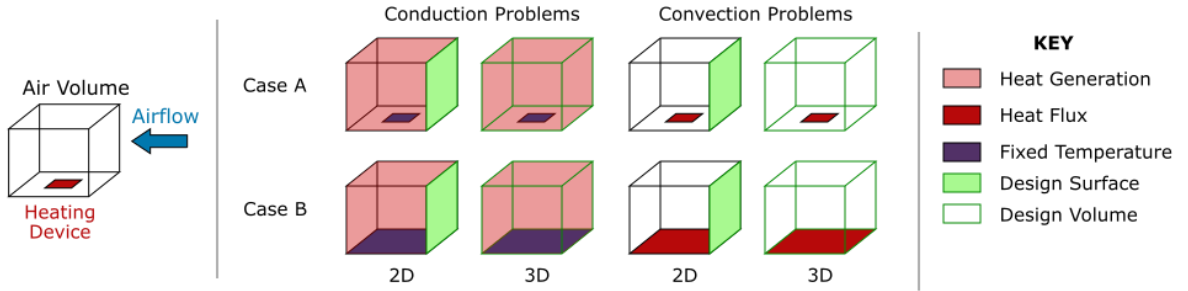


Figure 2. Heat sink design domain abstraction (left), reduced order analysis models (center), key (right).

For the analysis model, we consider three variations based on heat conduction. The first is a pure conduction formulation, where the input device heat flux is set as a heat generation in the design volume. The device surface is set as a fixed temperature constraint and the remaining boundaries are considered adiabatic such that all of the heat flux exits through the fixed temperature boundary. This analysis method is an abstraction of the convection problem in the reverse direction, moving heat from a volume to a surface. The second analysis strategy incorporates reduced-order convection considerations. Here the device heat generation is set as an input heat flux to the bottom surface of the design domain. The remaining boundaries are set as adiabatic such that the heat flux must be from within the domain. For one analysis formulation, an artificial convective force is applied uniformly on the domain. In the final analysis formulation, an artificial convective force is applied at the interface of solid and void material, defined by elements with partial density [3].

In addition to general physics considerations, several other analysis formulation features are varied. Two boundary condition sizes, including the true device size, Case A, and a simplified size, Case B, are utilized. Both 2D and 3D design problem applications are investigated. In the case of 2D design, the surface perpendicular to the airflow is selected as the design domain. For the 3D design problems, the entire bounding box of the air volume is used as the design domain. The design optimization problem can be formalized as:

$$\begin{aligned}
 & \min_{\mathbf{d}} \quad \Theta(\mathbf{d}) \\
 & \text{s. t.} \quad V(\mathbf{d}) \leq V_{\max} \\
 & \quad \quad R(\mathbf{d}) \geq R_{\min} \\
 & \quad \quad 0 \leq \mathbf{d} \leq 1,
 \end{aligned} \tag{1}$$

where some objective function,  $\Theta$ , is optimized with respect to the particular design variables for a given method. This is subject to two constraints: 1) the volume of conductive material  $V(\mathbf{x})$  is restricted to 50% of the domain volume, and 2) the radius of a fin  $R(\mathbf{x})$  is restricted to 0.5 mm. The minimum radius constraint is based on the manufacturing limitations at ShapeWays.com for silver material. The design vector and constraint implementation depend on the design method used, and will be discussed in the next section. For the heat spreading structure design tasks, we consider several candidate objective functions related to electronics applications, listed in Table 1.

Table 1. Candidate optimization objective functions.

$\Theta(\mathbf{d}) = \int_{\Omega} q \nabla T d\Omega$ (2)	$\Theta(\mathbf{d}) = \ T\ _p$ (3)	$\Theta(\mathbf{d}) = \frac{1}{n} \int_{\Omega} (T - T_{av})^2 d\Omega$ (4)
Thermal Compliance	Maximum Temperature	Temperature Variance

These include thermal compliance, which is related to energy minimization, maximum temperature (approximated using a p-norm function), and temperature variance, which quantifies the change in the temperature across the domain. The objectives presented here will be used to in separate optimizations for all combinations of design considerations.

### 3. Design Methodologies

#### 3.1 SIMP Method

The first method uses a voxel-based design representation. This method is adapted from [6], and structured for heat transfer applications. The design vector using this method is given by:

$$\mathbf{d} = [\alpha_1, \alpha_2, \dots, \alpha_n], \quad (5)$$

where each finite element (voxel) is assigned a density scalar,  $\alpha_i$ . The minimum radius constraint may be enforced implicitly using a density filter [9]. The volume constraint is calculated as the sum of element densities, and is enforced using an optimization constraint. This problem is solved using the Method of Moving Asymptotes (MMA) algorithm.

#### 3.2 Geometric Projection Method

This next method is based on the use of discrete geometric bars to represent the heat sink design. A differentiable geometric projection is used to map the bars onto the finite element mesh, as defined in [7]. This differentiable projection enables representation of the heat sink by simple geometry without the need to remesh the structure. The smooth projection also naturally accommodates the simplified convective boundary conditions used in this research. The composition of the design vector for this method follows:

$$\mathbf{d} = [x_{i1} \ y_{i1} \ x_{f2} \ y_{f2} \ \alpha_1, \dots, x_{in} \ y_{in} \ x_{fn} \ y_{fn} \ \alpha_n], \quad (6)$$

where each bar has a total of 5 design variables to capture the initial bar node,  $[x_{i1}, y_{i1}]$ , final bar node  $[x_{f2}, y_{f2}]$ , and bar density parameter,  $\alpha$ . In this study, a total of 10 bars are projected onto the domain. The minimum radius constraint is implicitly satisfied as the bars are fixed to the minimum radius size. The volume constraint is can be satisfied by removing and/or overlapping bars during the optimization routine. This optimization using this design representation is driven by the MMA algorithm.

#### 3.3 Space Colonization Method

This final method used for heat sink design is based on the use of generative algorithm as an indirect representation of the heat sink design. The generative algorithm used here is the Space Colonization Algorithm, which is used to emulate venation. This algorithm has shown promise in previous heat sink design studies [8], and the readers are referred to this document for details on the algorithm implementation. The composition of the design vector follows:

$$\mathbf{d} = [n_{\text{stems}}, n_{\text{stages}}, l_{\text{step}}, ax_1 \ ay_1, ax_2 \ ay_2, \dots, ax_n, ay_n], \quad (7)$$

where the optimizer will decide the number of initial stem nodes,  $n_{\text{stems}}$ , the number of venation growth stages,  $n_{\text{stages}}$ , the length of the vein growth per iteration,  $l_{\text{step}}$ , and the auxin coordinates  $[ax, ay]$ . For this study, the number of stems is varied from 1:10, the number of growth stages is varied from 1 to 3, the vein growth length is between 5-10% of the domain width, and 40 auxins are introduced on the domain. The same differential geometric projection as mentioned for the geometric projection method is applied to project the topology here on the finite element mesh with elements of a fixed width. A nested optimization loop is run for each design candidate to increase the projected bar widths uniformly until the minimum volume constraint is satisfied using a bisection algorithm. The outer loop topological design is driven by a genetic algorithm.

## 4. Optimization Results

Optimization was performed for each of the physics models, boundary conditions, optimization methods, and objective functions to result in 54 optimized heat spreader designs. A selection of the optimized designs is presented here to reveal particular trends. In Fig. 3, thermal compliance optimized designs for the conduction problem using various design method are presented. The best performing design was obtained using the space colonization algorithm, the second best by the geometric projection method, and the lowest-performing design was obtained via SIMP.



Figure 3. Topology optimization solutions for thermal compliance. SIMP method (left), space-colonization algorithm (center), geometric projection method (right).

When switching between physics analysis style, clear changes in structure can be seen. Consider the thermal compliance solutions using the SIMP approach shown in Fig. 4. The conduction physics presents a dendritic structure as typically seen in the literature. When including a constant convection term, a straight fin structure is preferred. When using the boundary-dependent convective heat flux term, pointed fins are generally formed.



Figure 4. SIMP topology optimization solutions for thermal compliance objective. Pure conduction (left), conduction with uniform convection (center), conduction with boundary-dependent convection (right).

As expected, the choice of objective function also resulted in significant changes in the topology structure of the optimized designs, as illustrated in Fig. 5. It was observed that, when moving from left to right in Fig. 5, the solutions become less bulky near the heat sink and feature more thin branches from left to right.

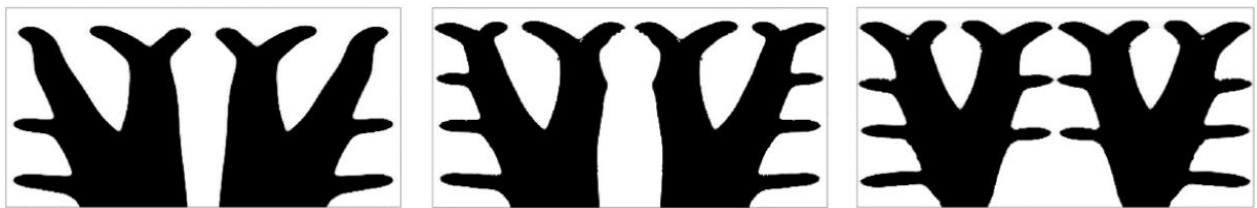


Figure 5. Topology optimization solutions for various objective functions. Thermal compliance (left), maximum temperature (center), temperature variance (right).

Of the optimized designs, 12 were selected and fabricated using a lost wax casting approach from the online vendor ShapeWays. These designs were then used for experimental validation.

## 5. Experimental Evaluation

To measure the performance of the optimized heat spreading structure, an experiment was designed. A custom PCB test coupon was made where a SiC device is soldered onto the top side of the board, and heat spreading devices are fixed onto the reverse side, as illustrated in Fig. 6. To minimize the thermal resistance between the SiC device and the heat spreading structure, Liquid Pro thermal interface material is applied between the PCB and the heat spreading structure. The experimental setup is shown in the center image, where a FLIR T450 camera is used to measure the maximum temperature at the center of the SiC device. A blower fan is set to a fixed power to force air through the heat spreading structure. To identify the best-performing heat spreading structure, the input power of the device will be increased incrementally and the maximum temperature of the SiC device is measured for each power level. The physical testbench and a sample thermal image is presented in the right image.

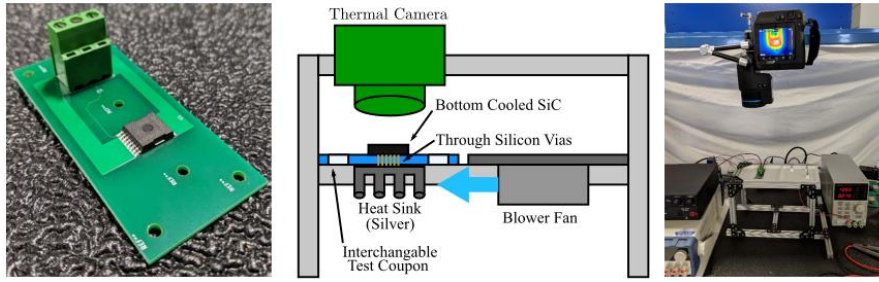


Figure 6. Experimental setup.

The maximum electronic device temperature, at 20W of power loss, for each heat spreading structure is presented in Fig. 7. A large difference, >30C, in performance from the best to worst design is measured. There does not appear to be any correlation relating the boundary conditions when designing for a cross-section perpendicular to the airflow. Furthermore, there does not appear to a correlation comparing the use of a conduction or convection model. On average, it appears that the variation objective performs well, and that the simple geometric projection method is effective at representing and accessing high-performance designs.

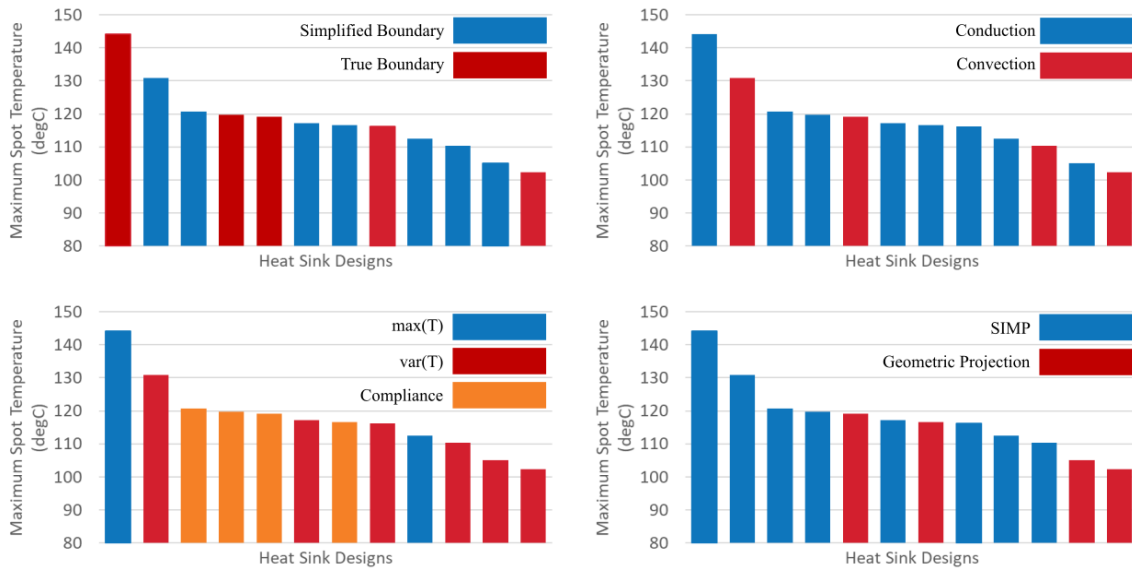


Figure 7. Complete experimental results compared by maximum temperature.

Analyzing the best few designs, several conclusions can be drawn, summarized in Fig. 8. The best designs have very similar slender fin features independent of design method used. Though the projection method produced the best two structures, the SIMP method also converged to a straight-fin structure. All three of the design methods were obtained using the variance objective function. The best design features a radial fin structure and provides a small performance improvement, ~3 degC, over the straight-fin structures.

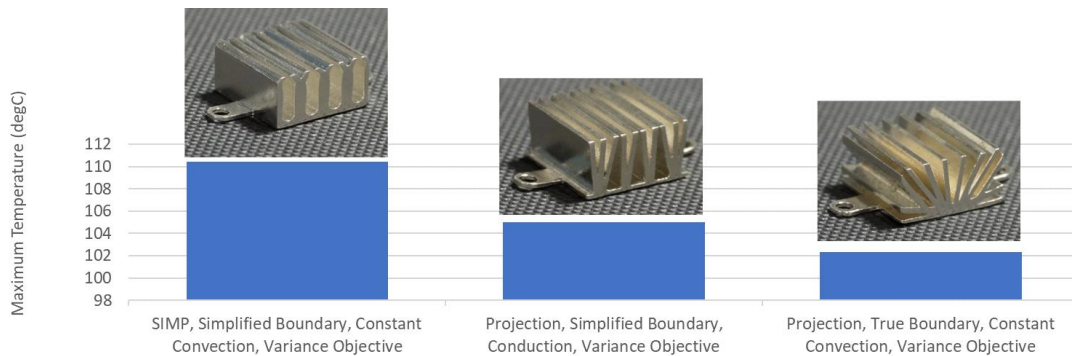


Figure 8. Best experimental results from manufactured designs. Maximum device temperature for 20W of loss presented.

Within the set of fabricated designs were structures with similar radial fins, shown in Fig. 9. The left structure had a maximum temperature of 114 °C, and the right structure had a maximum temperature of 102 °C. Though these heat spreading structures look similar at a glance, there are subtle, but important, geometric differences near the heat source. The best performing structure features some bulk conductive material near the heat source, which may help more effectively distribute the heat flux to the fins. This observation can be used to select good starting points for future optimization studies.

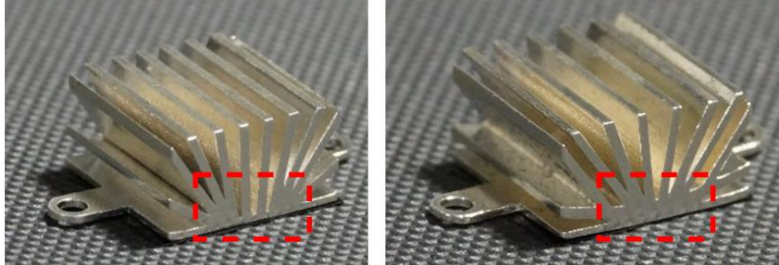


Figure 9. Optimized structure comparison. Average performing structure (left), best performing structure (right). Region of interested is highlighted in the dashed box, where the best design features some bulk material.

### 3. Conclusions

Based on the numerous design studies and experimental validation, several observations can be made. Foremost, the reduced-order physics models do not provide a consistent correlation with true system performance. Furthermore, adding flexibility in the design space did not result in heat spreader performance improvement. This may be due to the local nature of gradient-based algorithms. Lamellar structures produced by the geometric projection method seemed to perform well in practice for this application. The true optimal heat spreader for this application likely features some bulk material near the heating device, and some arrangement of radial fins. Formally investigating the effect of increasing design complexity is left as a topic of future work.

### Acknowledgments

This work was supported by the National Science Foundation Engineering Research Center for Power Optimization of Electro-Thermal systems (POETS) with cooperative agreements EEC-1449548.

### References

1. Alexandersen J, Sigmund O, Aage N. Large Scale Three-Dimensional Topology Optimisation of Heat Sinks Cooled by Natural Convection. *International Journal of Heat and Mass Transfer*, 2016, 100:876–891
2. Ramphueiphad S, Bureerat S. Synthesis of Multiple Cross-Section Pin Fin Heat Sinks Using Multiobjective Evolutionary Algorithms. *International Journal of Heat and Mass Transfer*, 2018, 118:462–470
3. Iga A, Nishiwaki S, Izui K, Yoshimura M. Topology optimization for thermal conductors considering design-dependent effects, including heat conduction and convection. *International Journal of Heat and Mass Transfer*, 2009, 52:2721-2732
4. Zhou M, Alexandersen J, Sigmund O, Pedersen C W B. Industrial application of topology optimization for combined conductive and convective heat transfer problems. *Structural and Multidisciplinary Optimization*, 2016, 54: 1045-1060
5. Dbouk T. A review about the engineering design of optimal heat transfer systems using topology optimization. *Applied Thermal Engineering*, 2017, 112: 841-854
6. Bendsøe MP, Kikuchi N. Generating Optimal Topologies in Structural Design Using a Homogenization Method. *Computer Methods in Applied Mechanics and Engineering*, 1988, 71(2):197–224
7. Norato J A, Bell B K, Tortorelli D A. A geometry projection method for continuum-based topology optimization with discrete elements. *Computer Methods in Applied Mechanics and Engineering*, 2015, 293: 306-327
8. Lohan D J, Dede E M, Allison J. Topology Optimization for Heat Conduction Using Generative Design Algorithms. *Structural and Multidisciplinary Optimization*, 2017, 55(3): 1063-1077
9. Bruns TE, Tortorelli DA. Topology optimization of non-linear elastic structures and compliant mechanisms, *Comput Methods in Appl Mech Eng*, 2001, 190(26-27), 3443–3459